Journal of Magnetism and Magnetic Materials 471 (2019) 400–405

Contents lists available at ScienceDirect

Journal of Magnetism and Magnetic Materials

journal homepage: www.elsevier.com/locate/jmmm

Research articles

Self-assembly of hen egg white lysozyme fibrils doped with magnetic particles

Jozefína Majorošová[a], Natália Tomašovičová[a,*], Veronika Gdovinová[a], Chih-Wen Yang[b], Marianna Batkova[a], Ivan Batko[a], Mária Demčaková[a], Kornel Csach[a], Martina Kubovčíková[a], Shura Hayryan[b], Ing-Shouh Hwang[b], Chin-Kun Hu[b,c,d], Peter Kopčanský[a]

[a] Institute of Experimental Physics SAS, Watsonova 47, 040 01 Košice, Slovakia
[b] Institute of Physics, Academia Sinica, 128 Section 2, Academia Rd., Nankang, Taipei 11529, Taiwan
[c] National Centre for Theoretical Sciences, National Tsing Hua University, Hsinchu 30013, Taiwan
[d] Department of Physics, National Dong Hwa University, Hualien 97401, Taiwan

ARTICLE INFO

Keywords:
Magnetic nanoparticles
Amyloid fibrils
Self-assembly
Birefringence

ABSTRACT

In this work, the interaction between spherical magnetic nanoparticles and amyloid fibrils as well as formation of self-assembled structures during drying process of such colloidal system were investigated. The final self assembled structures were observed experimentally by atomic force microscopy, scanning electron microscopy and polarizing microscopy. Our results show that the colloidal composites are self-assembled into flower-like patterns after the evaporation of liquid drop. These observations show that a large scale and well-organized multi-branched aggregates are formed during the process of drying. Moreover, observation by polarizing microscopy under crossed polarizers showed birefringence.

1. Introduction

Self-assembly of molecules is obvious in natural systems and therefore it is basis for the formation of diverse and complex biological structures [1]. There exists many ways how to obtain self-assembly or various patterns formation process onto a solid surface [2,3]. This effect may be either due to direct adsorption of the particles on the surface [4–6] or it can be the result of the evaporation of the solvent from the liquid drop [7–9]. Evaporation of solvent can be an important access to induce kinetically stable assemblies of building blocks with a large-scale specific arrangement [10]. In nature the process of self-assembly is governed by intra- and inter-molecular forces that lead molecules into a stable and low energy state. The mentioned forces include electrostatic interaction, hydrogen bonding, hydrophophic interactions and van der Waals forces. By combination of these forces together as a whole, it is possible to obtain structural conformation of all biological macromolecules and influence their interaction with other molecules as well [1]. The structure of the deposit can have various patterns from coffee drops [11] to more complex aggregates like fractal patterns [12] due to the physical and chemical processes that are involved during evaporation. Proteins are known to form highly complex of self-assembly patterns, for example: concentric rings, treelike fractals or dendrites by using salt-induced molecular self-assembly and droplet evaporation methods [13]. Understanding the mechanism of supramolecular assembly of small particles to form larger structures leads to potential application in materials engineering, where self-assembly into well-structured complexes can be used to fabricate advanced materials.

Amyloid fibrils have an important role in nanotechnology and biomaterials applications due to their unique physical and mechanical properties [14,15]. The most used and well characterized model protein for *in vitro* study of amyloid fibrillation is Hen egg white lysozyme (HEWL) that represents a structural homologue of human lysozyme. Magnetic nanoparticles (MNPs) are currently used in biomedical applications such as magnetic resonance imaging, drug delivery or even hyperthermia [16–19]. Nanoparticles may influence not only the formation, but also the structural stability of protein amyloid aggregates. The powerful tool is using MNPs and magnetic field as an organizing medium to induce the assembly of amyloid fibrils. Bolisetty and coworkers [20] have demonstrated the possibility to orient amyloid fibrils of β-lactoglobulin with MNPs under an external magnetic field due to adsorption of magnetic nanoparticles on fibril surface. In our previous works [21,22] the adsorption of MNPs on lysozyme amyloid fibrils (LAF) was observed where the adsorption was concentration dependent. The controlled self-assembly of lysozyme fibrils into micro-scale

* Corresponding author.
E-mail address: nhudak@saske.sk (N. Tomašovičová).

https://doi.org/10.1016/j.jmmm.2018.09.109
Received 12 June 2018; Received in revised form 19 September 2018; Accepted 28 September 2018
Available online 29 September 2018
0304-8853/

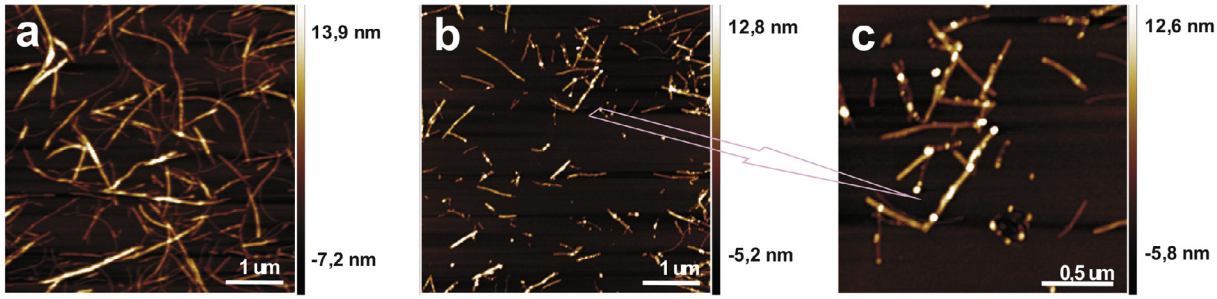

Fig. 1. Representative AFM images of (a) pure amyloid fibrils and (b) amyloid fibrils with magnetic nanoparticles, (c) the detail of the image (b).

structure with magnetic nanoparticles under the application of magnetic field is crucial for the study of their collective properties. Magnetic nanoparticles as a template for self-assembly of lysozyme fibrils represent an important tool for the achievement of various MNPs-based facilities [23]. The dynamic of forming dendritic structures during drying process was studied in our previous work by N. Tomasovicova, et al. [24]. In this work, we report detailed study of flower-like dendritic structures obtained by self-assembled suspension of lysozyme amyloid fibrils with the magnetic nanoparticles. The final structure was observed by polarizing microscopy (PM), atomic force microscopy (AFM) and scanning electron microscopy (SEM). These experimental techniques were used for better characterization of topography and morphology of dendritic structure as well as their building blocks. The influence of salt on the formation of dendritic structure as well as optical properties of such bio-hybrid structure were also studied.

2. Materials and methods

Hen egg white lysozyme (HEWL) (lyophilized powder, lot number L6876, 50,000 units mg 1 protein) was obtained from Sigma-Aldrich Chemical Company (St Louis, MO). All other chemicals were obtained from Sigma or Fluka and were of analytical reagent grade. Lysozyme amyloid fibrils were prepared by dissolving of HEWL powder to obtain a final concentration of 10 mg/ml in 0.2 M glycine-HCl buffer with pH 2.2 and 80 mM NaCl. Prepared solution in enclosed bottle was heated for 2 h at 65 °C with constant stirring speed of 250 rpm.

The magnetite nanoparticles were prepared by co-precipitation method [25]. The synthetized magnetic nanoparticles were washed by magnetic decantation several times to remove impurities produced during the precipitation process. After that the nanoparticle dispersion was stabilized by addition of perchloric acid; in acidic medium Fe_3O_4 nanoparticles are positively charged and ClO_4^- species are adsorbed on their surface. This ensures the electrostatic repulsion between the nanoparticles and thus the stability of prepared magnetic fluid. Electrostatically stabilized MNPs were dispersed in water to obtain magnetic fluid (MF). The mean hydrodynamic diameter of nanoparticles d = 26 nm was determined by dynamic light scattering using Zetasizer Nano ZS by Malvern Instruments (Germany). The value of polydispersity index was 0.26. Such magnetic fluids were used for preparation of mixture with amyloids.

Magnetic fluid with concentration of MNPs of 28 mg/ml was added to the initial solution of lysozyme amyloid fibrils (sLAF) with concentration of 10 mg/ml to achieve a ratio between volume of sLAF and MF solutions (V_{sLAF}: V_{MF}) in the mixture: 1 ml: 0.1 ml. The final concentration of MNPs in prepared solution was 2.8 mg/ml.

The ζ-potentials for individual sample were measured by Laser Doppler Electrophoretic measurement using Zetasizer Nano ZS by Malvern Instruments (Germany). Measurements were done at temperature 20 °C.

AFM topographic images of sLAF and mixture of sLAF and MNPs on mica were acquired in tapping mode at ambient conditions with a commercial beam-deflection AFM (Veeco di Innova, Bruker AXS Inc., Madison) using silicon AFM probes with a gold coating of the cantilever backside. The samples were prepared by drop casting of solution on the surface of freshly cleaved mica. They were rinsed with ultrapure water after 5–10 min of adsorption to remove redundant sample. Then the samples were left to dry before scanning.

Optical imaging, AFM and SEM observation of dendritic structures obtained by drying process were performed on the same sample. The solution was dropped on the glass slide and left to dry. Dried sample was observed first by optical microscopy followed by AFM. Before SEM imaging, a thin layer of Au was applied on prepared sample. Optical imaging was observed with the polarizing microscope Nikon Eclipse LV100 under bright field, using lenses of 10×, 20× and 50× magnifications. AFM observation was performed using Agilent 5500 AFM system equipped by PicoView 1.14.3 control software. The topography images were acquired in the tapping mode with standard silicon cantilevers with nominal resonant frequency of 300 kHz and nominal spring constant of 26 N/m (Olympus, model OMCL-AC 160TS). Images were processed using freely available software from Gwyddion (http://gwyddion.net). Scanning electron microscope (SEM) Tescan-VEGA3 LMU was used for morphological description of sample to see the structures at higher resolution. All measurements were carried out at ambient temperature in air, while relative humidity was in the range of 30–40%. The polarization dependent experiments were carried out by the same polarizing microscope with the possibility to vary the polarizer axis by 360° in order to analyse the transmitted intensity as a function of angle between the polarizer axis and orientation of the structures. The sample was diluted ten times and deposed on the glass slide.

3. Experimental results and discussion

Fig. 1 shows AFM images of pure sLAF and sLAF doped with MNPs. From the AFM images, it can be seen the typical amyloid morphology that confirm strongly the elongated character of the studied aggregates. The adsorption of MNPs on LAF clarifies interaction activity between these two components. The study of interactions of different nanoparticles such as iron oxide, Ag and Au with different proteins as β-lactoglobulin, insulin and lysozyme [26–28] showed the adhesion of nanoparticles on the fibril surfaces. These results are in excellent agreement with our results and can be observed in bulk samples.

The forces of electrostatic interaction as well as van der Waals represent two types of binding forces that take action in the interplay between the protein fibrils and MNPs [29]. The attractive protein-protein interactions should exist to initiate the self-organization of proteins. The isoelectric point, that represents the pH value at which the ζ-potential value is zero due to the no electric charge on the surface of a particle, of HEWL is 11.35 and therefore, at pH 2.2 the protein is positively charged. The positive ζ-potential for our sLAF of 38.7 mV has been confirmed. Accounts on that, the protein molecules repulse each other due to the same-charge exclusion effect. However, different situation is in the case of Fe_3O_4 MNPs, where the ζ-potential depends on pH. The positive ζ-potential was observed at pH<6.3, while at pH>6.3 is

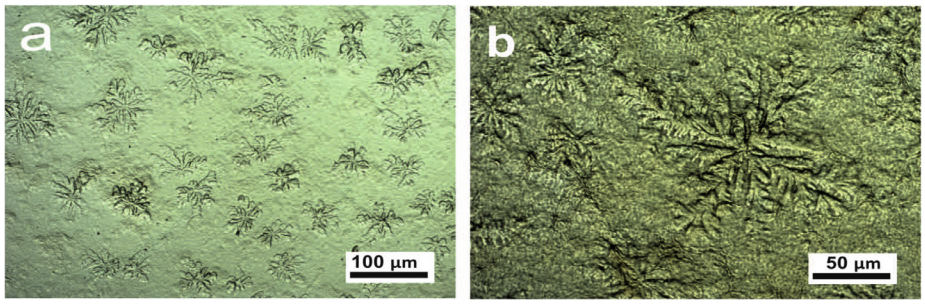

Fig. 2. Flower-like dentritic structure observed by polarizing microscope at magnification (a) 10× and (b) 20×.

negative [30]. Our results showed that spherical MNPs are positively charged (the ζ-potential is 43 mV) and therefore, the electrostatic interactions would cause repulsion between the fibrils and the surface of particles. Nevertheless, it has been shown experimentally that spherical MNPs adsorb to LAF, and our assumption is that this phenomenon is governed rather by the van der Waals forces instead of electrostatic interactions. Similar results were also observed in experimental work by Chen et al. [26], where they studied interactions of insulin proteins with iron nanoparticles.

The self-assembly process of protein was studied across various length scales, by using optical microscopy (millimetres), atomic force microscopy and scanning electron microscopy (micrometres and nanometres). A small drop of prepared mixture was dropped onto the cleaned glass slide, and without rinsing was left there to dry in ambient atmosphere at room temperature. Finally, a protein pattern was obtained by gradually evaporating water.

After complete evaporation of water, the sample was first observed by polarizing microscopy. Fig. 2 shows bright field microscopy images of pared sample. The observed pattern showed highly ordered flower-shaped multi-branched nanostructures formed on the glass. The obtained structures did not pre-exist in solution, but they were formed after the deposition during the drying process. The detailed structure becomes apparent at higher magnification (see Fig. 2(b)).

To obtain details about the observed structures, SEM and AFM imaging of the same samples were performed (Fig. 3). While the AFM provides a three-dimensional picture of topography of the dendritic structure, the SEM technique shows lower magnification of the surface in two dimensions. Therefore, using these two techniques, which are complementary for high resolution surface investigations, gives a more complete "picture" of the observed sample. The addition of MNPs favours the self-organization of protein at an early stage, which eventually leads to the formation of regular protein patterns.

Fig. 4 shows AFM images of dendritic structure under various magnifications. It has been found that the structures appear in patterns of snowflake consisting of many small aggregates.

A profile analysis shown in Fig. 5 shows detailed height image and three-dimensional picture with their corresponding topography. The analysis showed that building block of final structure are much larger than single MNPs. These results suggests that they are formed from aggregates of MNPs and proteins.

A closer observation of the morphology by SEM reveals that the micropattern of mixture is formed from MNPs conjugated with sLAF. The branches are extending in various directions with equal growth of the dendritic arms (see Fig. 6(a) and (b)). Fig. 6(c) shows detail of the center of the dentritic structure. A significant precipitated salt was observed around the dendrites structure (see Fig. 6(c) and (d)). Fibrils as well as pure particles were not observed. We expect, that together with magnetic nanoparticles they form building blocks and they have changed their structure to form dendrites. As was shown in work by G. Chen and G.J. Mohamed [31] the presence of salt play important role in the process of dendritic structures formation. Fig. 7(a) shows polarizing microscopy image of dried buffer containing salt, Fig. 7(b) the solution of LAF doped with magnetic nanoparticles, and Fig. 7(c) the solution of LAF doped with magnetic nanoparticles prepared in buffer without salt. From Fig. 7 is seen that pure salt precipitate in cubic structure which can serve as a nucleus for dendritic structures forming. In the sample without salt, the formation of dendritic structures was not observed. Moreover, formation of ring from MNPs was observed during drying process. Such behaviour is typical for colloidal fluids [11]. However, the "coffee ring" was not observed in the sample containing salt, what suggest that MNPs are incorporated to the building blocks which form dendritic structure.

The radially-branched-dendritic structures of prepared samples may be described by theoretical model on the random aggregation of solid particles into branched structures called the classical diffusion limited aggregation (DLA) theory [32]. On drying, hen egg lysozyme spontaneously forms branched patterns that are similar to the fractal structures formed by a DLA [33] that has been observed in the assembly of materials like colloids, polymer thin films [34] or peptides [33]. Therefore, the DLA may be regarded as a model of random irreversible growth, starting from seed particles. Such seed acts as the centre of the cluster nucleation. By random-walking a second particle is attached to

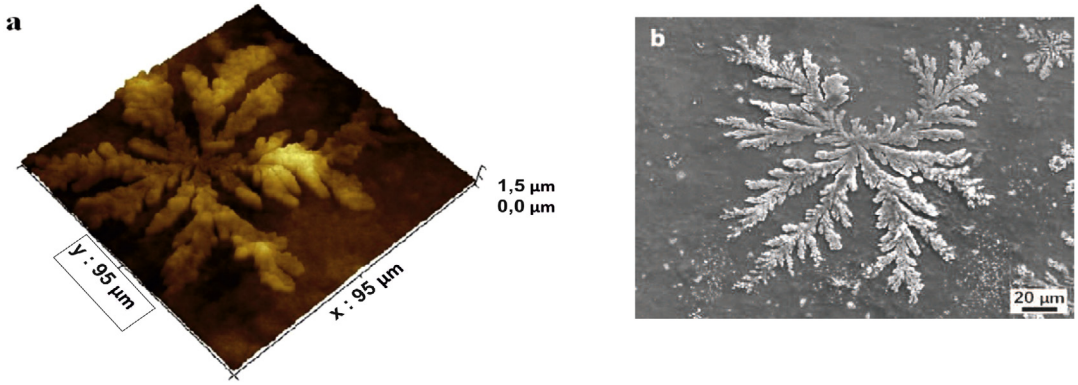

Fig. 3. Representative (a) AFM image of the flower-like pattern and (b) SEM image of the same sample.

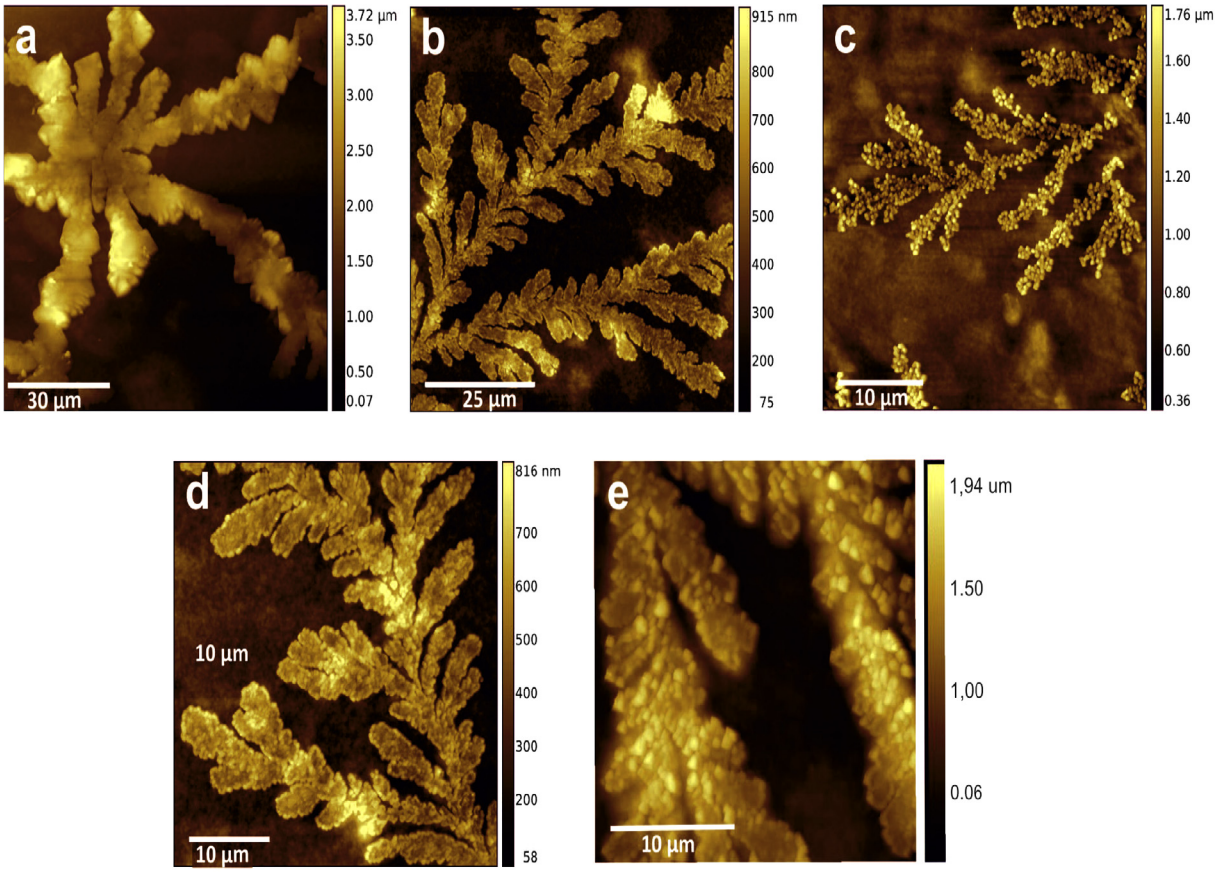

Fig. 4. Representative AFM image of the (a) dendritic centre, (b)–(d) the branches of dendritic structure, and (e) the details of dendritic arms.

the seed. It sticks and forms a 2-particle cluster system that extends the initial seed. By further repeating of this process one observes the growth of a random object [35]. Fractal structures formed mostly by DLA have the property of being devoid of any directional characteristic. Therefore, branches seem to grow out in random directions, where the final obtained structures are too organized and well formed.

To investigate the birefringence properties of prepared mixture, the final solution was diluted ten times, deposed on the glass, left to dry and then observed under crossed polarizers by PM. Fig. 8 shows image of dry sample under observed by polarizing microscope. When sample was viewed in polarized light, the resulting images showed lightly birefringent structures with changing colours by changing the angle of polarizers even without the Congo red. This assay is usually used for detecting the presence of amyloids by monitoring the characteristic

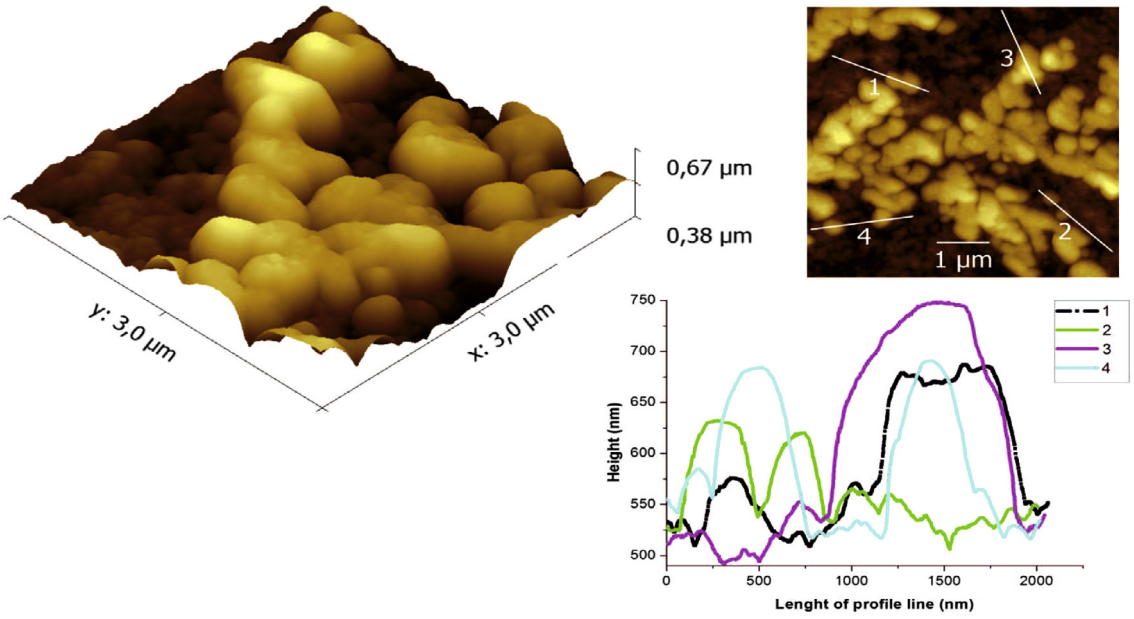

Fig. 5. Representative AFM image of the dendritic building blocks in 3D structure and their corresponding topographies.

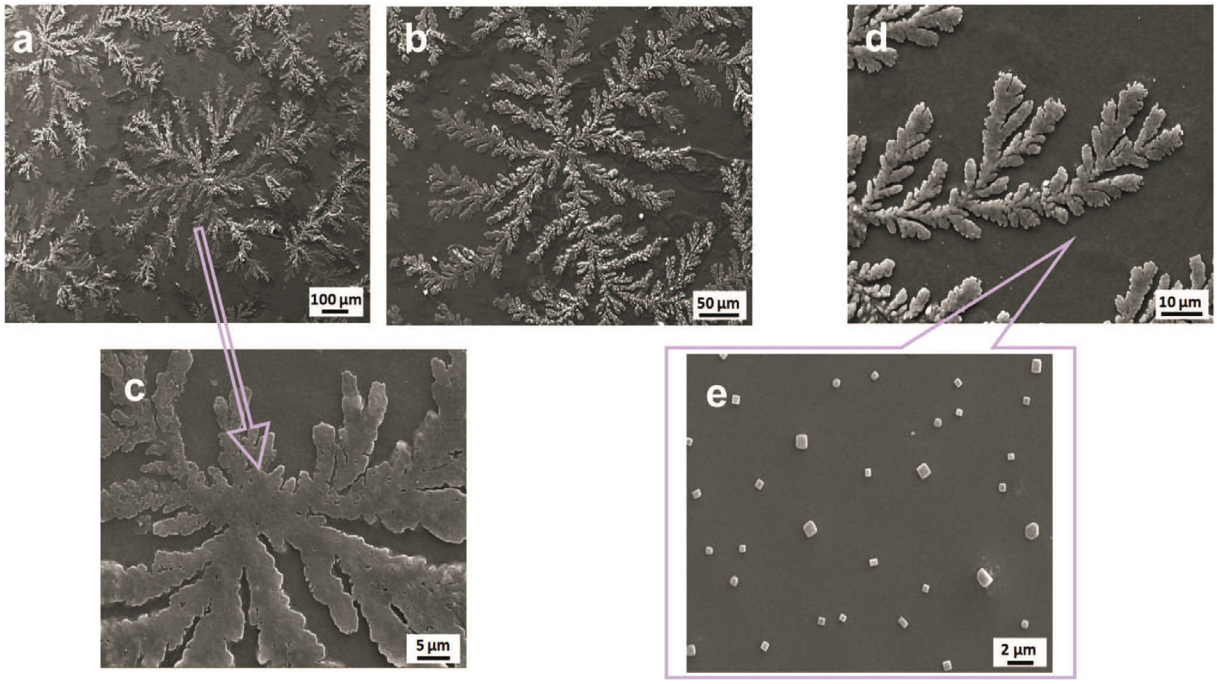

Fig. 6. Representative SEM image of (a) and (b) flower-like structure, (c) detail of the centre, (d) detail of arm, and (e) the precipitates of crystallized salt present among dentritic branches.

yellow-green birefringence under crossed polarizers [36–38]. The colour of the background and dendritic structure were changed due to the changes in mutual orientation of the optical axes (polarizer and analyzer are no longer perpendicular).

Fig. 8(a) and (c) show parallel polarized images of dendritic structure, and Fig. 8(b) and (d) are the cross polarized images of Fig. 8(a) and (c) obtained by rotating the polarizer 90°. The birefringence pattern of the sample clearly shows the existence of a large number of microdomains with random orientation of the green-blue and yellow protein domains. The branches of dendrites change from dark (Fig. 8(b)) to bright (Fig. 8(a)) when the polarizing angle is changed. Importantly, crystallization started from the bottom of the sample at the glass-protein interface that leads to forming large, well-organized layers with uniforms blue and yellow coloration. Therefore, we assume that the brightness of the patterns and their coloration is proportional to the degree of protein solidification in the sample. This phenomenon is typical characteristic of anisotropic microstructures and is not observed in pure magnetic particles neither in pure lysozyme. Polarization dependent experiments demonstrate that the formed bio-hybrid dendrites possess the properties of crystallinity and birefringence and moreover, they are magnetically active due to presence of magnetic nanoparticles.

4. Conclusion

Self-assembled dendritic patterns of solution with magnetic nanoparticles and lysozyme amyloid fibrils on the glass surface from evaporating drops have been observed by various visualisation techniques. The observed micro-structured protein patterns were governed by the protein concentration and solvent evaporation at ambient conditions. As shown by AFM and SEM techniques, the interconnected aggregates form complex surface patterns. Colloidal nanocrystals are of special interest in construction of ordered assemblies to be used in optoelectronics, photonics and biosensing. It is important that the nanocrystal properties essential to allow the arrangement process, including their size, shape, surface protection, stabilization and charge, can be controlled along with the electronic structure of each nanocrystal. The birefringence and crystallinity of the formed dendritic structures was confirmed by polarizing microscopy. It was shown in several works [39–42] that the mixture of protein with magnetite nanoparticles has potential applications in nanomedicine, biomedical engineering, pharmaceutical fields or industrial technology. Comprehensive understanding of their interactions and structuralization is therefore very significant. Different physical parameters, such as drop volume, using temperature controlled drying, size of the particles as well as the concentration of protein, may also affect the self-assembly structures.

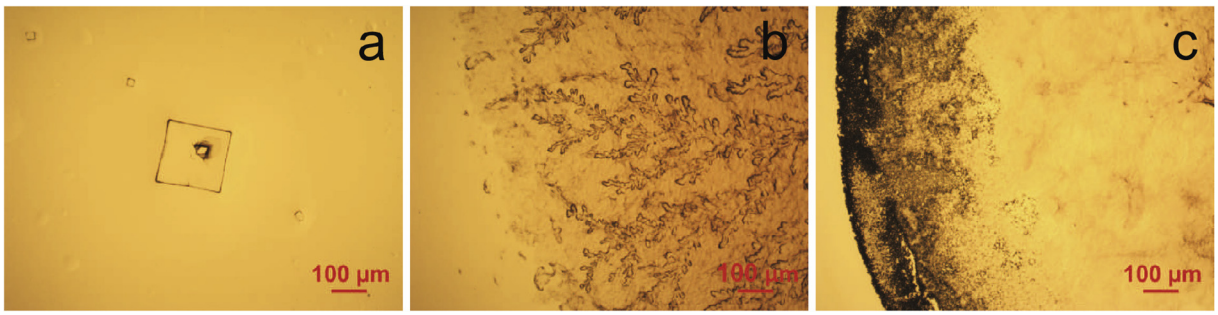

Fig. 7. Polarizing microscopy image of dried (a) buffer containing salt, (b) solution of LAF doped with magnetic nanoparticles in buffer with salt and (c) solution of LAF doped with magnetic nanoparticles in buffer without salt.

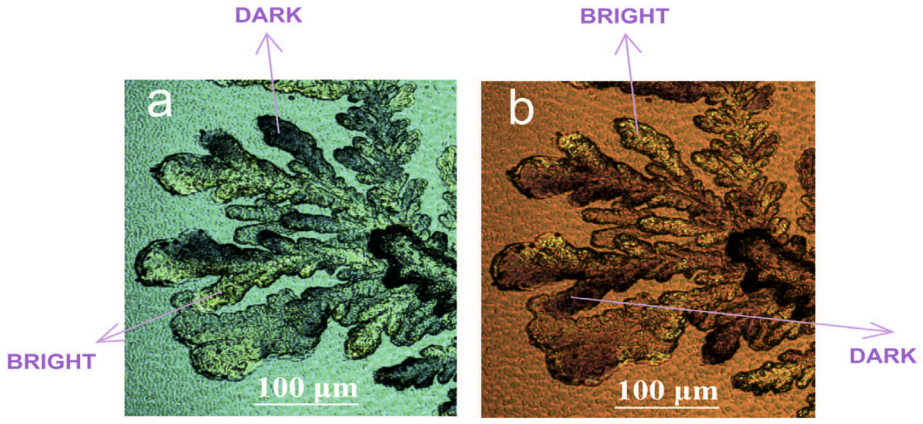

Fig. 8. Polarizing microscopy image of ten times diluted solution of the initial mixture with ultrapure water. (a) parallel polarized images of dendrites, and (b) corresponding cross polarizing images recorded with 90° rotation of polarizer.

Understanding the key parameters, which govern the formation of these structures may provide an interesting route for the controlled elaboration of complex and fractal surface assemblies. We believe that this experimental work in the long run will help by the construction of dynamically self-assembled protein-magnetic materials, which can be managed using external magnetic field to required localities and will allow controlled capture and delivery of nanosized cargo.

Acknowledgements

This work was supported by the Slovak Academy of Sciences, in the framework of projects VEGA 2/0016/17, the Slovak Research and Development Agency under the contract No. APVV- 015-0453, Ministry of Education Agency for Structural Funds of EU in frame of project 26210120012, SH and CKH were supported in part by the grant MOST 104-2923-M-001-004, CKH was also supported in part by Grants MOST 106-2112-M-001-027 and MOST 107-2112-M-259-006.

References

[1] S.G. Zhang, Nat. Biotechnol. 21 (2003) 1171.
[2] H. Haidara, L. Vonna, L. Vidal, Macromolecules 43 (2010) 2421–2429, https://doi.org/10.1021/ma902363p.
[3] Á. Marín, H. Gelderblom, D. Lohse, J. Snoeijer, Phys. Rev. Lett. 107 (2011) 085502, https://doi.org/10.1103/l.107.085502.
[4] S. Sahoo, S. Husale, B. Colwill, T.-M. Lu, S. Nayak, P.M. Ajayan, ACS Nano 3 (2009) 3935, https://doi.org/10.1021/nn900915m.
[5] F. Bai, C. Zeng, S. Yang, Y. Zhang, Y. He, J. Jin, Biochem. Biophys. Res. Commun. 369 (2008) 830–834, https://doi.org/10.1016/j.bbrc.2008.02.085.
[6] M.A. Ray, N. Shewmon, S. Bhawalkar, L. Jia, Y. Yang, E.S. Daniels, Langmuir 25 (2009) 7265–7270, https://doi.org/10.1021/la900257p.
[7] R. Bhardwaj, X. Fang, P. Somasundaran, D. Attinger, Langmuir 26 (2010) 7833–7842, https://doi.org/10.1021/la9047227.
[8] E. Bormashenko, G. Whyman, R. Pogreb, O. Stanevsky, M. Hakham-Itzhaq, O. Gendelman, Isr. J. Chem. 47 (2007) 319–328, https://doi.org/10.1560/IJC.47.3-4.319.
[9] H.-P. Cong, S.-H. Yu, Curr. Opin. Colloid Interface Sci. 14 (2009) 71–80, https://doi.org/10.1016/j.cocis.2008.09.003.
[10] D. Gentili, G. Foschi, F. Valle, M. Cavallini, F. Biscarini, Chem. Soc. Rev. 41 (2012) 4430–4443.
[11] R.D. Deegan, O. Bakajin, T.F. Dupont, G. Huber, S.R. Nagel, T.A. Witten, Nature 389 (1997) 827–829, https://doi.org/10.1038/39827.
[12] K. Mougin, H. Haidara, Langmuir 18 (2002) 9566–9569, https://doi.org/10.1021/la020491w.
[13] S. Kyle, A. Aggeli, E. Ingham, M.J. McPherson, Trends Biotechnol. 27 (2009) 423–433, https://doi.org/10.1016/j.tibtech.2009.04.002.
[14] I. Cherny, E. Gazit, Angew Chem. Int. Ed. Engl. 47 (2008) 4062–4069, https://doi.org/10.1002/anie.200703133.
[15] T.P. Knowles, T.W. Oppenheim, A.K. Buell, D.Y. Chirgadze, M.E. Welland, Nat. Nanotechnol. 5 (2010) 204–207, https://doi.org/10.1038/nnano.2010.26.
[16] M. Namdeo, S. Saxena, R. Tankhiwale, M. Bajpai, Y.M. Mohan, S.K. Bajpai, J Nanosci Nanotechnol. 8 (2008) 3247, https://doi.org/10.1166/jnn.2008.399.
[17] M. Johannsen, U. Gneveckow, L. Eckelt, A. Feussner, N. Waldofner, R. Scholz, S. Deger, P. Wust, S.A. Loening, A. Jordan, Int. J. Hyperthermia 21 (2005) 637, https://doi.org/10.1080/02656730500158360.
[18] C. Sun, J.S. Lee, M. Zhang, Adv. Drug Deliv. Rev. 60 (2008) 1252, https://doi.org/10.1016/j.addr.2008.03.018.
[19] N. Kohler, C. Sun, A. Fichtenholtz, J. Gunn, C. Fang, M. Zhang, Small 2 (2006) 785, https://doi.org/10.1002/smll.200600009.
[20] S. Bolisetty, J.J. Vallooran, J. Adamcik, R. Mezzenga, ACS Nano 7 (2013) 6146–6155, https://doi.org/10.1021/nn401988m.
[21] J. Majorosova, V.I. Petrenko, K. Siposova, M. Timko, N. Tomasovicova, V.M. Garamus, M. Koralewski, M.V. Avdeev, B. Leszczynski, S. Jurga, Z. Gazova, S. Hayryan, C.K. Hu, P. Kopcansky, Colloids Surf. B: Biointerfaces 146 (2016) 794.
[22] V. Gdovinová, N. Tomašovičová, I. Batko, M. Batková, L. Balejčíková, V.M. Garamus, V.I. Petrenko, M.V. Avdeev, P. Kopčanský, J. Magn. Magn. Mater. 431 (2017) 8.
[23] A. Sukhanova, Y. Volkov, A.L. Rogach, A.V. Baranov, A.S. Susha, D. Klinov, V. Oleinikov, J.H.M. Cohen, I. Nabiev, Nanotechnology 18 (2007) 185602.
[24] N. Tomašovičová, P.S. Hu, C.L. Zeng, M. Huráková, K. Csach, J. Majorošová, M. Kubovčíková, P. Kopčanský, Colloids Surf. B: Biointerfaces 161 (2018) 457–463.
[25] R. Massart, IEEE Trans. Magn. 17 (1981) 1247, https://doi.org/10.1109/TMAG.1981.1061188.
[26] Y.W. Chen, C.W. Chang, H.S. Hung, M.L. Kung, B.W. Yeh, S. Hsieh, Nanotechnology 27 (2016) 415702, https://doi.org/10.1088/0957-4484/27/41/415702.
[27] Y. Kim, J.H. Park, H. Lee, J.M. Nam, Sci. Rep. 6 (2016) 19548.
[28] S. Bolisetty, J.J. Vallooran, J. Adamcik, R. Mezzenga, ACS NANO 7 (2013) 6146.
[29] W. Wu, X. Sun, Y. Yu, J. Hu, L. Zhao, Q. Liu, Y. Zhao, Y. Li, Biochem. Biophys. Res. Commun. 373 (2008) 315, https://doi.org/10.1016/j.bbrc.2008.06.03.
[30] B. Wang, F. Zhang, J. Qiu, X. Zhang, H. Chen, Y. Du, P. Xu, Acta Chimica Sinica 67 (2009) 1211.
[31] G. Chen, G.J. Mohamed, Eur. Phys. J. E 33 (2010) 19, https://doi.org/10.1140/epje/i2010-10649-4.
[32] T.A. Witten, L.M. Sander, Phys. Rev. Lett. 47 (1981) 1400, https://doi.org/10.1103/PhysRevLett. 47.1400.
[33] A. Lomander, W.M. Hwang, S.G. Zhang, Nano Lett. 5 (2005) 1255, https://doi.org/10.1021/nl050203r.
[34] G. Reiter, I. Botiz, L. Graveleau, N. Grozev, K. Albrecht, A. Mourran, M. M'ller, Lect. Notes Phys. 714 (2007) 179, https://doi.org/10.1007/3-540-47307-6.
[35] R. Srivastava, P.K. Srivastava, Adv. Nat. Sci.: Nanosci. Nanotechnol. 5 (2014) 015018, https://doi.org/10.1088/2043-6262/5/1/015018.
[36] R. Khurana, V.N. Uversky, L. Nielsen, A.L. Fink, J. Biolog. Chem. 276 (2001) 22715–22721, https://doi.org/10.1074/jbc.M011499200.
[37] P.K. Teng, D. Eisenberg, Protein Eng. Des. Sel. 22 (2009) 531–536, https://doi.org/10.1093/protein/gzp037.
[38] A.J. Howie, D.B. Brewer, D. Howell, A.P. Jones, Laboratory Investigation 88 (2008) 232–242, https://doi.org/10.1038/labinvest.3700714.
[39] R. Raliya, T.S. Chadha, K. Hadad, P. Biswas, Curr Pharm Des. 22 (2016) 2481, https://doi.org/10.2174/1381612822666160307151409.
[40] S. Bucak, D.A. Jones, P.E. Laibinis, T.A. Hatton, Biotechnol. Progress 19 (2003) 477, https://doi.org/10.1021/bp0200853.
[41] M.A. Busquets, R. Sabate, J. Estelrich, Nanoscale Res Lett. 9 (2014) 538, https://doi.org/10.1186/1556-276X-9-538.
[42] M. Zaman, E. Ahmad, A. Qadeer, G. Rabbani, R.H. Khan, Int. J. Nanomedicine 9 (2014) 899, https://doi.org/10.2147/IJN.S54171.